Electromagnetic phenomena in heterogeneous media: Effective properties and local behavior

Electromagnetic phenomena in heterogeneous media: Effective properties and local behavior

Oriano Bottauscio[a] and Alessandra Manzin
Istituto Nazionale di Ricerca Metrologica, Strada delle Cacce 91, I-10135 Torino, Italy

Valeria Chiadó Piat and Marco Codegone
Dipartimento di Matematica, Politecnico di Torino, Corso Duca degli Abruzzi 24, I-10129 Torino, Italy

Mario Chiampi
Dipartimento di Ingegneria Elettrica, Politecnico di Torino, Corso Duca degli Abruzzi 24, I-10129 Torino, Italy

(Received 4 April 2006; accepted 22 June 2006; published online 17 August 2006)

The purpose of this paper is the use of a mathematical homogenization approach based on the multiple scale expansion theory for modeling the electromagnetic phenomena arising in heterogeneous media under an imposed magnetic flux. The attention is focused on the analysis and discussion of the merits and limits of this theoretical approach in reproducing not only the effective macroscopic properties but also the local behavior, under a wide frequency range and considering different constitutive and geometrical parameters. The results show that the proposed method is able to predict local and integral physical quantities, ranging from a substantially global behavior in the whole media to significantly localized effects determined by the microscopic structure. © *2006 American Institute of Physics*. [DOI: 10.1063/1.2234816]

I. INTRODUCTION

Heterogeneous media are commonly adopted for electromagnetic applications in many branches of industry and science due to their ability to be tailored to meet specific requirements. Among them, a class of materials is constituted by composite dielectrics, which are promising because unique combinations of dielectric parameters, different from the ones of the basic constituents, can be obtained. In magnetic applications, heterogeneous media range from composite magnetic materials, prepared by dispersing metal powders in a homogenous dielectric lattice, to sintered materials, with permeable and conductive grains insulated through layers generated by an oxidation process, to packaged media, where magnetic thin ribbons are assembled to obtain a global ensemble. Examples of such media are the sintered or ferrite magnetic cores and the strip-wound amorphous cores, commonly employed for applications in the frequency range up to some megahertz.

Limiting the attention to magnetic materials, a relevant aspect is the appearance of induced conductive and displacement currents, which affect the effective properties of the macroscopic media. The circulation of these currents is strongly determined by the fine-scale structure of the heterogeneous media. The fine-scale structure has a stochastic character in composite and sintered magnetic materials, while a regular character is found when dealing with packages of amorphous ribbons. In the first case, a random field approach should be adopted in principle, introducing statistical properties at microscopic level. Alternatively, taking into account the high number of particles randomly dispersed in the lattice, the stochastic structures can also be reasonably reduced to fine-periodic ones.

The research topic, which focuses on the determination of the effective properties of composite materials starting from the characteristics of the ensemble of particles dispersed in a given lattice, has a long tradition beginning with the work by Rayleigh in 1892.[1] In this work, an exact formula was derived for the determination of the effective dielectric constant when a regular ensemble of conductive spheres is dispersed in a rectangular lattice. Successively, Lam[2] extended the approach to include eddy current effects in the determination of the effective permeability of a cubic lattice of conductive magnetic spheres. Starting from the paper of Garnett[3] other significant works have focused the attention on modeling the stochastic structures of composite materials, considering the interaction of randomly dispersed particles.[4–6]

More recently, also thanks to the computational power increase, the modeling of the electromagnetic behavior of heterogeneous media has been faced by numerical approaches instead of analytical formulas.[7–11] The advantage with respect to analytical approaches is the possibility of extending the model applicability to the analysis of more complex structures. As a drawback, their application to the study of two-dimensional or even more to three-dimensional domains rapidly leads to exorbitant computational burdens, if one expects to introduce a spatial discretization of the fine-periodic structure, keeping contemporary into account the macroscopic domain boundaries. This drawback can be overcome assuming an infinite periodicity, reducing the analysis to a single cell with periodic boundary conditions, but in this case edge effects in the macroscopic behavior are intrinsically neglected.

[a]Electronic mail: botta@inrim.it

A rationale of most of the works devoted to modeling heterogeneous media in electromagnetics is the determination of the global properties of the macroscopic media, while less attention is paid to the possibility of reproducing the local behavior of the electromagnetic field quantities. In this paper, we are interested in modeling the electromagnetic phenomena in heterogeneous media with the aim of reproducing both the effective macroscopic properties and the local behavior. To do this, we make use of a mathematical homogenization approach, based on the multiple scale expansion theory, applied to the Helmholtz equation. Following this approach, the field equations are handled introducing a solution in terms of an asymptotic form, with a zero-order term and higher-order correctors. The first item represents the homogenized solution, which is the solution in a homogenous medium with "averaged" properties; the other terms provide corrections able to reproduce the local behavior of the heterogeneous material. The application of the homogenization theory to elliptic partial differential equations, in different fields of physics, has been found very promising, as detailed in several works, see, for example, Refs. 12–18.

In order to analyze and discuss in detail the potentialities of the proposed mathematical approach to handle heterogeneous electromagnetic media, the attention is focused on two categories of problems with a deterministic character. In the first one a two-dimensional isotropic or anisotropic structure is considered, while in the second one the analysis is focused on a two-dimensional layered structure with spatial periodicity along one direction. In both cases the electromagnetic phenomena are evaluated when a magnetic flux flows along the orthogonal direction. In all problems, the use of the homogenization theory provides very accurate results both concerning integral and local quantities, with a significant reduction of the computational burden with respect to the standard approaches able to account for local heterogeneities.

II. SETTING OF THE PROBLEM

Let us consider a two-dimensional bounded domain S in $\Re^2$, with a coordinate system denoted by $s=(x_1,x_2)$, having associated unit vectors $(\mathbf{e}_1,\mathbf{e}_2)$. The domain is intersected by a known sinusoidal magnetic flux Φ (angular frequency ω) flowing along the normal direction (unit vector $\mathbf{e}_3$). Let the field quantity be denoted by $T(t)=\underline{T}e^{i\omega t}$ where $\underline{T}$ is a complex number (phasor), the governing equation, written in the harmonic domain, results

$$i\omega\mu[\underline{T}-M(\underline{T})]-div\left(\frac{1}{\sigma^*}\nabla\underline{T}\right)=-i\omega\frac{\mu}{m}\underline{\Phi}\quad\text{in } S,$$

$$\underline{T}(s)=0\quad\text{on } \partial S. \tag{1}$$

In (1) $\underline{T}=(0,0,\underline{T}(s))$ is the electric vector potential, i is the imaginary unit, $\mu=\mu(s)$ is the magnetic permeability, $\sigma^*=\sigma(s)+i\omega\varepsilon(s)$ is the complex conductivity, with σ the electrical conductivity and ε the dielectric constant, and $M(\underline{T})$ denotes the weighted average,

$$M(\underline{T})=\frac{1}{m}\int_S\mu\underline{T}ds\quad\text{with } m=\int_S\mu ds. \tag{2}$$

Both electric and magnetic properties are assumed to be isotropic.

Being that S is a highly periodic domain, from now on we shall assume that σ^* and μ are space periodic, with period $Y=]0,1[\times]0,1[$. In the following the spatial period Y of the domain will be defined as the elementary cell, with a local coordinate system $y=s/\eta=(y_1,y_2)$. By denoting the η-periodic functions $\sigma^*_\eta(s)=\sigma^*(s/\eta)$ and $\mu_\eta(s)=\mu(s/\eta)$, the aim is the determination of the asymptotic behavior of $\underline{T}_\eta$, solution of the problem

$$i\omega\mu_\eta[\underline{T}_\eta-M_\eta(\underline{T}_\eta)]-div\left(\frac{1}{\sigma^*_\eta}\nabla\underline{T}_\eta\right)=-i\omega\frac{\mu_\eta}{m_\eta}\underline{\Phi}\quad\text{in } S,$$

$$\underline{T}_\eta(s)=0\quad\text{on } \partial S, \tag{3}$$

as $\eta\to 0$.

III. HOMOGENIZATION

Considering the Hilbert space $H=H_0^1(S;\mathbf{C})$, the weak formulation of stationary problem (3), with test function ν, becomes

$$\int_S\frac{1}{\sigma^*_\eta}\nabla\underline{T}_\eta\cdot\nabla\nu ds+i\omega\int_S\mu_\eta(\underline{T}_\eta-M_\eta(\underline{T}_\eta))\nu ds$$
$$=-\frac{i\omega}{m_\eta}\int_S\mu_\eta\underline{\Phi}\nu ds\quad\text{for all } \nu\in H. \tag{4}$$

By applying Lax-Milgram theorem in the complex form[12] to Eq. (4), we obtain the existence and uniqueness of the solution $\underline{T}_\eta\in H$ satisfying an *a priori* estimate $\|\underline{T}_\eta\|\leqslant c$ with c independent of η. Hence, the passage to the limit $\eta\to 0$, allows us to obtain the "homogenized equation,"

$$\int_S A^0\nabla\underline{T}_0\cdot\nabla\nu ds+i\omega\int_S\mu^0[\underline{T}_0-M(\underline{T}_0)]\nu ds$$
$$=-\frac{i\omega}{m}\int_S\mu^0\underline{\Phi}\nu ds. \tag{5}$$

Here $\mu^0=\int_Y\mu dy$ and A^0 is, in the general case, a 2×2 tensor, whose elements a^0_{ij} are determined, following the energy method,[12] as

$$a^0_{ii}=\int_Y\frac{1}{\sigma^*}dy+\int_Y\frac{1}{\sigma^*}\frac{\partial w_i}{\partial y_i}dy\quad\text{with } i=1,2,$$

$$a^0_{12}=\int_Y\frac{1}{\sigma^*}\frac{\partial w_2}{\partial y_1}dy,\quad a^0_{21}=a^0_{12}. \tag{6}$$

Function $w_i\in H^1_{\text{per}}(Y)$ is a solution of the cell problem

$$\int_Y\frac{1}{\sigma^*}(\nabla w_i+\boldsymbol{e}_i)\cdot\nabla\nu dy=0\quad\text{with } i=1,2$$
$$\text{for all } \nu\in H^1_{\text{per}}(Y), \tag{7}$$

where $H^1_{\text{per}}(Y)$ denotes the periodic functions in $H^1(Y)$.

When considering elementary cells having geometrical symmetry with respect to both coordinate axes (y_1 and y_2) with origin in the cell center, it results that $a^0_{21}=a^0_{12}=0$. In this case the diagonal elements of $[A^0]^{-1}$ represent the homogenized complex electrical conductivity of the media along the two axes ($\sigma^0_{x1}+i\omega\varepsilon^0_{x1}, \sigma^0_{x2}+i\omega\varepsilon^0_{x2}$).

Making reference to a rectangular domain S, having dimensions $2a$ and $2b$, respectively, along x_1 and x_2 coordinates with origin in the center of the rectangle and provided that A^0 is a diagonal tensor, Eq. (5) has the following closed form solution:

$$\underline{T}_0 = \frac{\Phi}{\mu^0} \cdot \frac{(\underline{\mathfrak{I}}(x_1,x_2)-1)}{\int_S \underline{\mathfrak{I}}(x_1,x_2)ds}, \tag{8}$$

with

$$\underline{\mathfrak{I}}(x_1,x_2) = \frac{\cosh(\alpha x_2)}{\cosh(\alpha b)} + \sum_{k=1,3,\ldots,}^{\infty} P_k \cos\left(\frac{k\pi x_2}{2b}\right)\cosh(x_1\sqrt{\beta_k})$$

being

$$\alpha = \sqrt{i\omega\mu^0/a^0_{11}}, \quad \beta_k = \left[\alpha^2 + \left(\frac{k\pi}{2b}\right)^2\right]\frac{a^0_{11}}{a^0_{22}},$$

$$P_k = \frac{4\alpha^2}{k\pi\left[\alpha^2+\left(\frac{k\pi}{2b}\right)^2\right]}\frac{\sin(k\pi/2)}{\cosh(a\sqrt{\beta_k})}.$$

.

IV. ASYMPTOTIC EXPANSION

The solution $\underline{T}_0(s)$ of the homogenized equation (5) is the zero-order term of the asymptotic expansion of the true solution $\underline{T}_\eta$. As $\eta\to 0$ $\underline{T}_0$ is closed to the true solution $\underline{T}_\eta$. In presence of the preponderant local effects due to the microscopic structure, corrector terms are added to the zero-order solution in order to improve the approximation. A first-order corrector $\underline{T}_1(s,y)$ is defined as

$$\underline{T}_1(s,y) = w_1(y)\frac{\partial \underline{T}_0}{\partial x_1}(s) + w_2(y)\frac{\partial \underline{T}_0}{\partial x_2}(s). \tag{9}$$

It can be proved that $\|\underline{T}_\eta - (\underline{T}_0+\eta\underline{T}_1(s,y))\|_{H^1}\to 0$ and $\|\nabla\underline{T}_\eta - (\nabla\underline{T}_0+\nabla_y\underline{T}_1(s,y))\|_{L^2}\to 0$ as $\eta\to 0$.

A second-order corrector $\underline{T}_2(s,y)$ can be constructed as follows. Let us define by w_{ij} the periodic solution of the cell problem,

$$\int_Y \frac{1}{\sigma^*}\nabla w_{ij}\cdot\nabla\nu dy = \int_Y c_{ij}\nu dy \quad \text{with } i=1,2\ j=1,2 \quad \text{for all } \nu\in H^1_{\text{per}}(Y), \tag{10}$$

where the functions c_{ij} are defined by $c_{ij}=b_{ij}(y)-\int_Y b_{ij}dy$, with

$$b_{ij}(y) = \frac{\delta_{ij}}{\sigma^*} + \sum_{k=1}^{2}\left[\frac{\delta_{ik}}{\sigma^*} + \nabla_k w_j + \nabla_k\left(\frac{\delta_{ik}}{\sigma^*}w_j\right)\right] \tag{11}$$

being w_j the solutions of the cell problem (7).

Corrector $\underline{T}_2(s,y)$ is so defined as

$$\underline{T}_2(s,y) = \sum_{i=1}^{2}\sum_{j=1}^{2}\nabla_{ij}\underline{T}_0(s)w_{ij}(y) \tag{12}$$

and can be proved that $\|\underline{T}_\eta - (\underline{T}_0+\eta\underline{T}_1(s,y)+\eta^2\underline{T}_2(s,y))\|_{H^2}\to 0$ as $\eta\to 0$.

V. RESULTS AND DISCUSSION

The analysis developed in the present section aims at investigating the capability and the limits of the multiple scale expansion theory to reproduce the electromagnetic phenomena arising within a heterogeneous periodic structure, when a sinusoidal magnetic flux Φ is imposed to flow through its cross section S. An average magnetic flux density having a peak value of 10 mT is imposed in all the considered cases.

Two kinds of periodicity are taken into consideration. In the first case, the studied structures have a spatial periodicity along both coordinates x_1 and x_2, with square elementary cells constituted of a ferromagnetic inclusion (material A) located within a low conductivity lattice (material B) [see Fig. 1(a)]. This structure, which models an idealized ferrite or composite magnetic core,[19] can include isotropic (circular and square inclusions) or anisotropic (elliptical inclusion) cells. The ferromagnetic inclusions have a relative magnetic permeability $\mu_{rA}=100$ and an electrical conductivity $\sigma_A=10$ S/m, while the lattice has an electrical conductivity σ_B ranging from 10^{-4} to 10^{-2} S/m and a relative electric permittivity $\varepsilon_{rB}=10$.

The second studied structure is composed of a sequence of two layers with different electrical and magnetic properties [Fig. 1(b)]. This structure, with periodicity only along x_2 axis, can reproduce the cross section of a laminated or strip-wound magnetic core.[20] Ferromagnetic material C has relative magnetic permeability $\mu_{rC}=100$ and electrical conductivity $\sigma_C=10^6$ S/m, while material D is a low conductive medium with relative electric permittivity $\varepsilon_{rD}=10$.

In most of the examples, a structure with a limited number of cells (9×9) or layers (nine) is considered. The choice of performing computations with a limited number of elementary cells is justified by the possibility of comparing the results (eddy current distributions and Joule energy losses) with the ones provided by a standard finite element approach, where each single cell is discretized accounting for the different material properties.

The results put in evidence that, depending on the supply frequency and geometrical and constitutive properties of the components, the eddy current distributions range between two limit behaviors:

- a global behavior, where the eddy currents flow in the whole domain and the effects of the local heterogeneities are negligible;
- a local behavior where the phenomena are confined

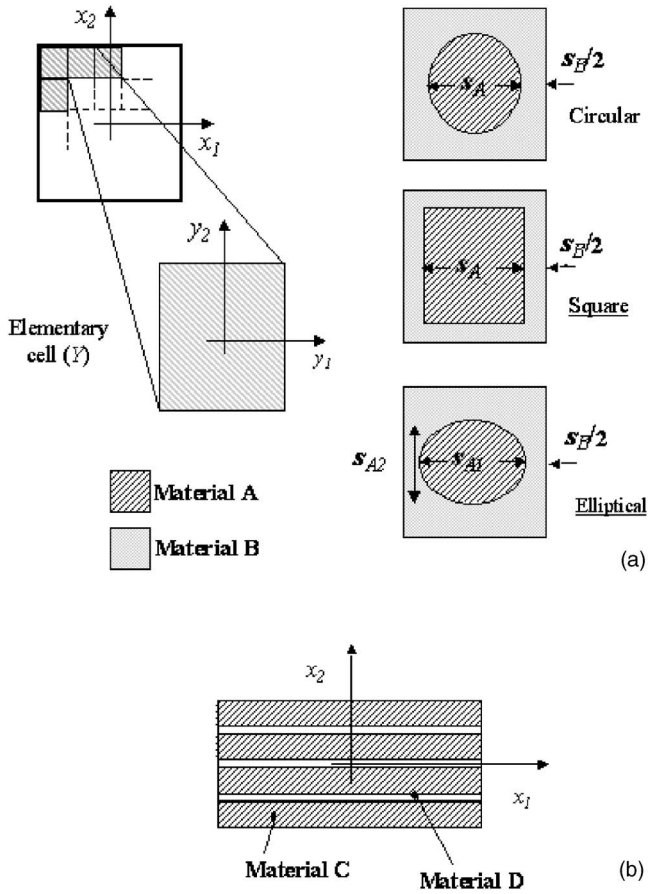

FIG. 1. Scheme of the two structures considered in the examples. Squared-pattern domain with a periodic structure along x_1 and x_2 coordinates (a), layered domain with a periodicity along x_2 coordinate (b). For the first structure, the dimensions of the inclusions and of the low conductivity material are indicated with s_A and s_B, respectively.

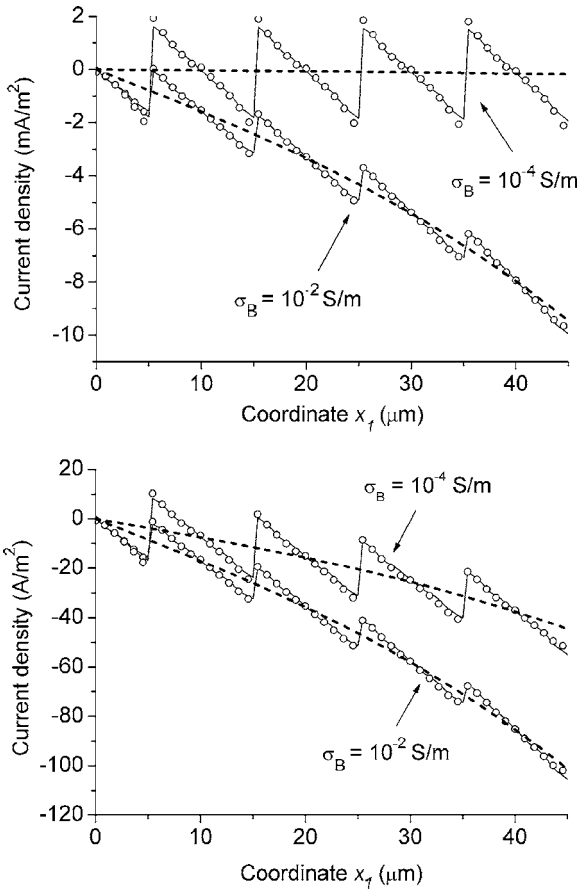

FIG. 2. Instantaneous current density distribution along x_1 axis considering square inclusions ($s_A = 10$ μm) within a lattice having $s_B = 100$ nm and two values of electrical conductivity ($\sigma_B = 10^{-2}$ S/m, $\sigma_B = 10^{-4}$ S/m). The supply frequencies are 1 kHz (a) and 10 MHz (b). In the diagrams, the solid lines represent the standard finite element solutions, the dot lines the solutions obtained with the homogenization approach considering higher order corrector terms, and the dashed lines the zero-order homogenization solutions.

within a single cell, without interactions with the nearest cells.

The results here obtained show that the multiple scale expansion theory is able to satisfactorily predict any behavior between the limit cases, provided that second order corrector terms are included in the computations.

A. Two-axis periodicity

The analysis is first developed on cells with square inclusions having a side of 10 μm, investigating, in particular, the influence of the conductivity and of the thickness of the low conductivity lattice. It must be noted that, due to the isotropic properties of the square, the diagonal elements of tensor A^0 are equal.

Assuming s_B equal to 100 nm, two values of conductivity σ_B (10^{-2} and 10^{-4} S/m) are considered. The instantaneous current density along x_1 is represented in Fig. 2, for 1 kHz and 10 MHz. The results provided by the homogenization approach are compared with the ones given by the standard finite element model of the heterogeneous domain. It must be pointed out that the finite element technique requires the solution of an algebraic system of ~20 000 unknowns, while the proposed method involves the solution of problems (7) and (10) with ~800 unknowns. The same figures also report the diagrams of the current density computed solving homogenized equation (5) without higher order correctors; these results, obtained assuming the domain as homogeneous, represent a good approximation, but the effects of local heterogeneities cannot be included. It is worth noting that in Fig. 2(a) the current density distribution for $\sigma_B = 10^{-4}$ S/m shows how the electromagnetic phenomena have assumed a prevalent local behavior, without influence of the macroscopic domain boundaries. This behavior is well evidenced by the comparison of the induced current distributions reported in Figs. 3(a) and 3(b). The field lines show how, increasing the frequency from 1 kHz to 10 MHz, the distribution changes from local to global.

The capability of the multiple scale expansion theory of reproducing the global and local phenomena is also confirmed by the diagrams of the Joule energy losses per unit volume (w) versus frequency presented in Fig. 4(a) ($\sigma_B = 10^{-2}$ S/m) and Fig. 4(b) ($\sigma_B = 10^{-4}$ S/m). In all the cases, the losses per unit volume in low conductive material B (w_B) are significantly higher than the ones in material A, even if their contribution on the total losses is weaker, due to the reduced volume of medium B. In Fig. 4(b) the predictions provided by two simpler models are also presented. The first

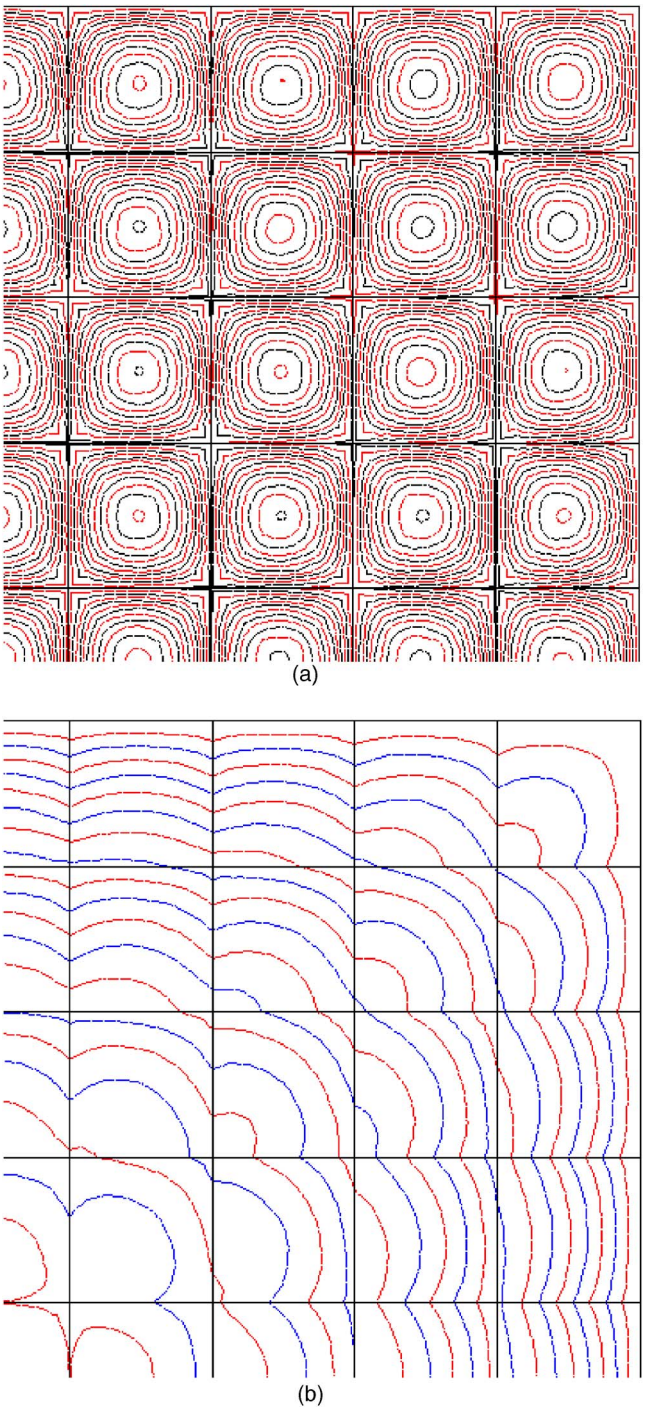

FIG. 3. Instantaneous induced current density distribution considering square inclusions ($s_A=10$ μm) within a lattice having $s_B=100$ nm and $\sigma_B=10^{-4}$ S/m. The supply frequencies are 1 kHz (a) and 10 MHz (b).

one, obtained neglecting higher order correctors, is suitable for modeling a global behavior. The second one derives from the field solution in a single cell with periodicity boundary conditions, and then it is able to reproduce a totally local behavior. This last model provides accurate predictions under low frequency supply, since the lattice behaves as a barrier towards eddy currents, which are mainly confined within the conductive inclusions. But, at higher frequencies, the increment of displacement currents determines diffusion over the whole domain, making the model with single cell periodicity unable to provide reliable results.

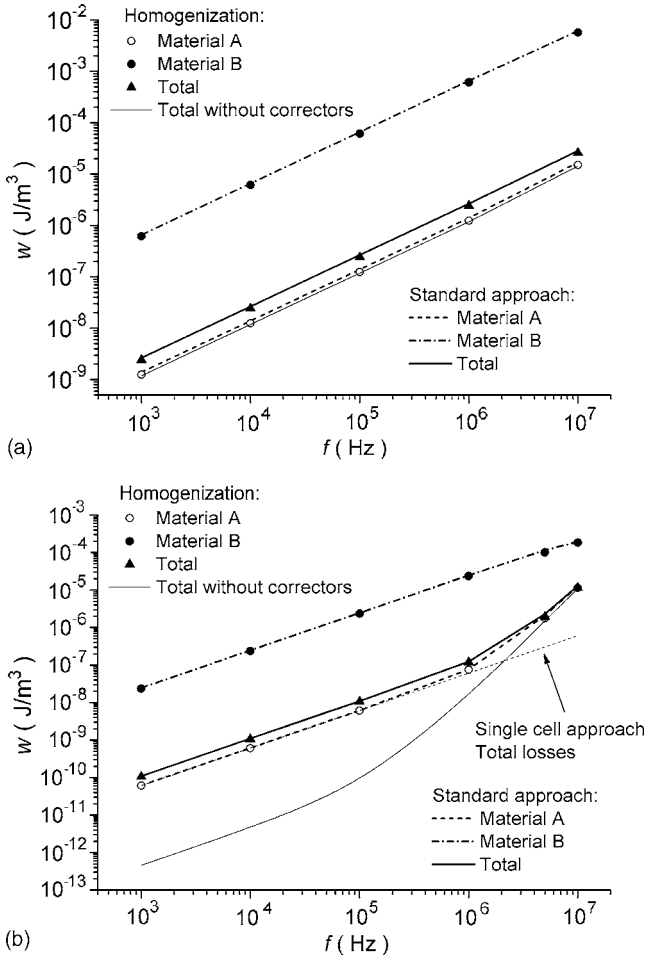

FIG. 4. Joule energy losses per unit volume versus frequency considering square inclusions ($s_A=10$ μm) within a lattice having $s_B=100$ nm. Two values of the electrical conductivity of the lattice are considered: $\sigma_B=10^{-2}$ S/m (a) and $\sigma_B=10^{-4}$ S/m (b).

The analysis is also performed to evaluate the influence of thickness s_B of the lattice separating adjacent cells, keeping the inclusion dimensions constant. As a general result, the Joule energy losses w reduce at the increase of s_B. This behavior is put in evidence in Fig. 5(a), where s_B is varied from 10 nm to 2 μm, with $\sigma_B=10^{-2}$ S/m and 10 MHz supply frequency. A similar effect is also found for the homogenized values of electrical conductivity ($\sigma^0_{x1}=\sigma^0_{x2}=\sigma^0$) and permittivity ($\varepsilon^0_{x1}=\varepsilon^0_{x2}=\varepsilon^0$), while homogenized magnetic permeability μ^0, which depends only on the ratio between the volumes of the two materials, has a linear behavior.

The influence on the Joule energy losses of the edge effects, due to the boundary of the macroscopic domain S, is finally investigated, varying the number of cells, whose dimension is kept fixed. Thus, an increase of the cell number corresponds to an enlargement of the domain S. The attention is focused on a supply frequency of 1 kHz, with a low electrical conductivity of the lattice ($\sigma_B=10^{-4}$ S/m and $\sigma_B=10^{-6}$ S/m), imposing the same value of the average magnetic flux density (10 mT). The Joule energy losses, plotted in Fig. 6 as a function of the domain dimension, show that at its increase the current field tends towards a global distribution with paths involving the whole domain. This behavior is proven by the fact that the computed losses approach the

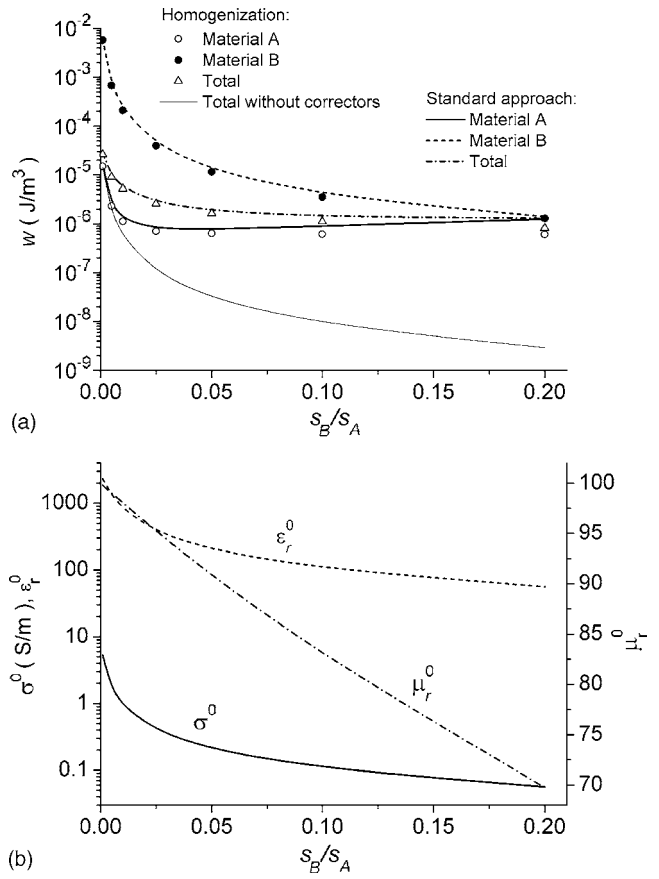

FIG. 5. Influence of thickness s_B for $\sigma_B=10^{-2}$ S/m at 10 MHz: Joule energy losses per unit volume (a) and homogenized parameters (b).

zero-order corrector solution. On the contrary, with smaller domain dimension the behavior tends to become strictly local, requiring the use of higher corrector terms for an accurate prediction of losses.

When considering circular inclusions, the phenomenon is always local due to the prevalent role of the low conductivity lattice on the field distribution. Figure 7 shows Joule energy losses per unit volume versus frequency in the case of circular inclusions of radius equal to 5 μm within a lattice having a minimum thickness $s_B=10$ nm and electrical conductivity $\sigma_B=10^{-2}$ S/m. In comparison with the standard finite element approach, multiple scale expansion method slightly underestimates losses for material A (inclusion) and overestimates losses for material B (lattice). Therefore, the total losses w are found to be lower than in the case of square inclusions with the same electromagnetic parameters.

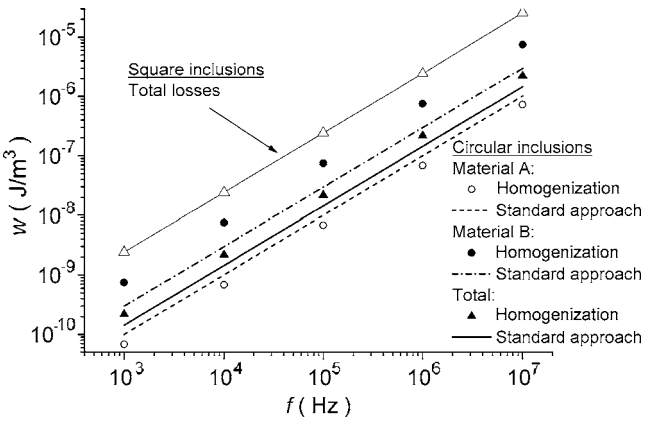

FIG. 7. Joule energy losses per unit volume versus frequency considering circular inclusions ($s_A=10$ μm) within a lattice having $s_B=100$ nm and $\sigma_B=10^{-2}$ S/m. The total losses for square inclusions are also reported for comparison.

The cells with elliptical inclusions are intrinsically anisotropic: Thus the diagonal elements of tensor A^0 are not equal and, consequently, the behaviors along x_1 and x_2 axes are different. In the computations, the major and minor axes of the ellipse are $s_{A1}=10$ μm and $s_{A2}=6.5$ μm, respectively; the minimum lattice thickness along x_1 axis is $s_B=1$ nm. As an example, Fig. 8 reports the instantaneous current density distributions along x_2 axis for $\sigma_B=10^{-2}$ S/m and $f=10$ MHz. The results show that the current density distribution, which has a prevalent local behavior, is not completely well reconstructed by the homogenization technique, also

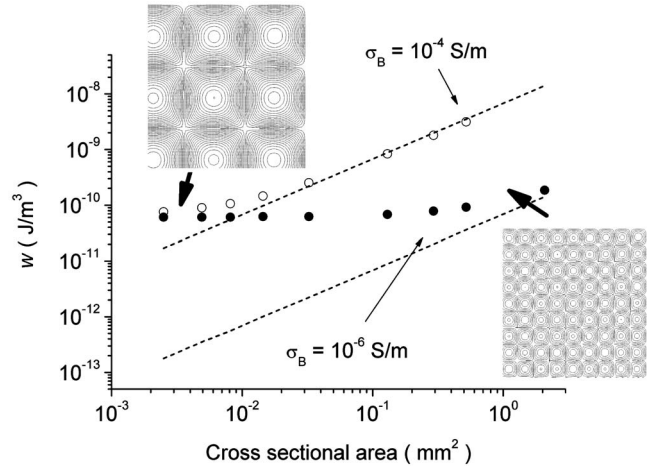

FIG. 6. Influence of the cross sectional area on Joule energy losses per unit volume considering square inclusions ($s_A=10$ μm) within a lattice having $s_B=100$ nm and two values of the electrical conductivity ($\sigma_B=10^{-4}$ S/m and $\sigma_B=10^{-6}$ S/m). In the diagrams, the dot represents the solutions obtained with the homogenization approach considering higher order corrector terms, while the dashed lines the zero-order homogenization solutions.

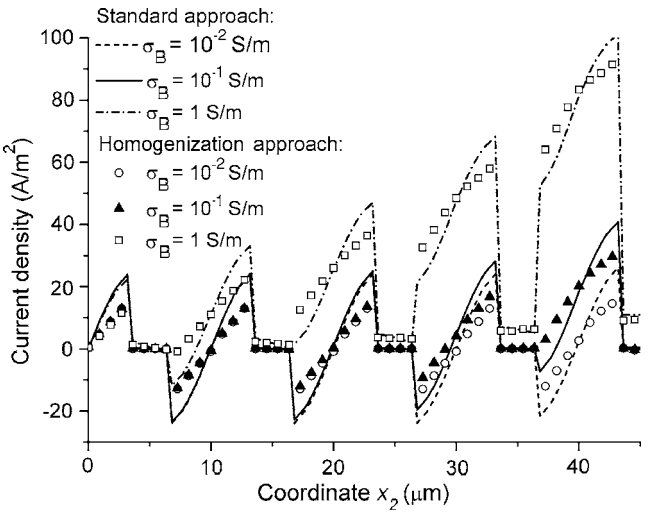

FIG. 8. Instantaneous current density distribution along x_2 axis considering elliptical inclusions ($s_{A1}=10$ μm, $s_{A2}=6.5$ μm) within a lattice having $s_B=1$ nm and three values of the electrical conductivity ($\sigma_B=10^{-2}-1$ S/m). The supply frequency is 10 MHz.

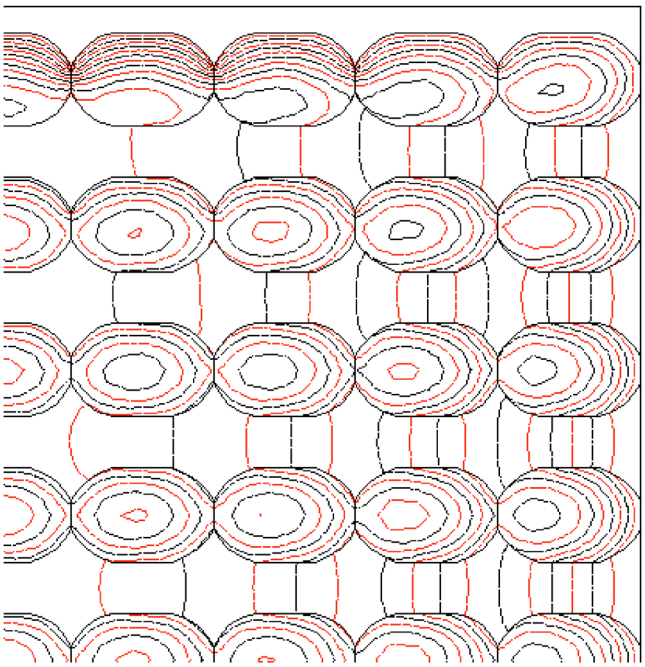

FIG. 9. Instantaneous induced current density distribution considering an elliptical inclusion ($s_{A1}=10$ μm) within a lattice having $s_B=1$ nm and $\sigma_B=10^{-2}$ S/m. The supply frequency is 10 MHz.

when the electrical conductivity σ_B is modified from 10^{-2} up to 1 S/m. The diagrams for the highest conductivity value evidences a more pronounced concentration of the current density towards the domain boundary, as confirmed by the corresponding instantaneous flux line distribution of Fig. 9. It is interesting to note that the value of σ_B significantly affects both homogenized electric conductivity along x_2 axis and homogenized electric permittivity along x_1 axis, while the other parameters practically do not change (see Fig. 10).

Finally in Fig. 11, the homogenized parameters are reported as a function of the ratio between the axes s_{A2} and s_{A1} of the elliptical inclusions. It is evident how the parameters along x_2 axis abruptly increase when the ratio s_{A2}/s_{A1} tends to 1, i.e., when the elliptical inclusion tends to a circular one.

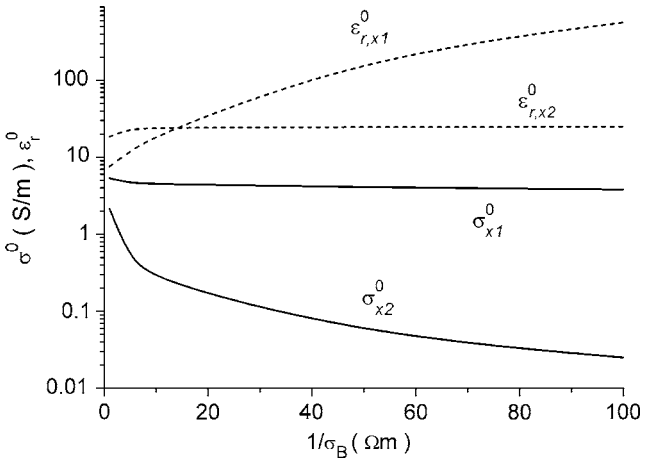

FIG. 10. Influence of the electrical conductivity σ_B on the homogenized parameters of a structure with elliptical inclusions. The supply frequency is 10 MHz.

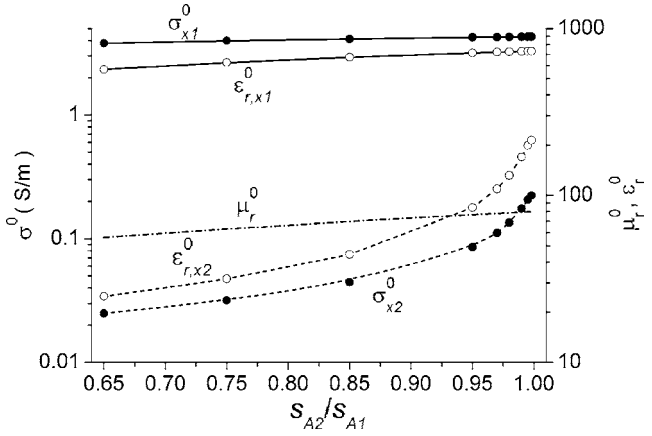

FIG. 11. Influence of the ratio s_{A2}/s_{A1} on the homogenized parameters at 10 MHz, for $s_B=1$ nm and $\sigma_B=10^{-2}$ S/m.

B. Uniaxial periodicity

The domain is the cross section of a core with nine ferromagnetic conductive laminations (material C) having thickness equal to 10 μm separated by a low conductive 100-nm-thick layer (material D).

In general, the computed behavior is similar to the one obtained for the two axial symmetry. As an example, Fig. 12 shows how, under 1 MHz supply frequency, an increase of the electric conductivity of material D from 10^{-4} to 10^{-2} S/m facilitates the flowing of eddy currents between laminations (interlaminar currents), concentrating the currents towards the boundaries. Also the Joule energy losses per unit volume versus frequency show an evolution similar to the one obtained considering cells with square inclusions, with the highest values in the low conductivity medium (see Fig. 13).

VI. CONCLUSIONS

In this paper the electromagnetic phenomena in heterogeneous media, constituted of a periodic microscopic struc-

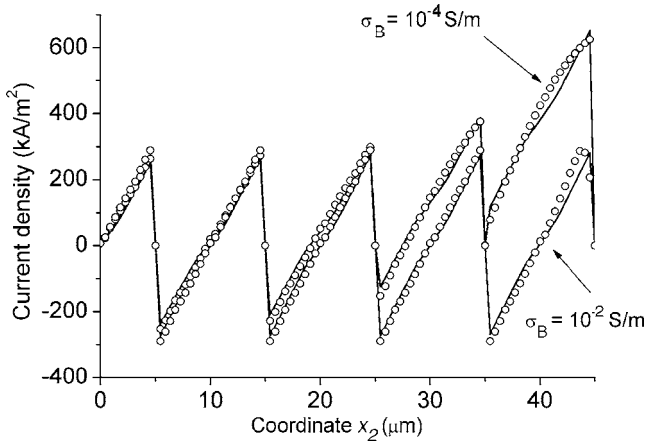

FIG. 12. Instantaneous current density distributions along x_2 axis for two values of the electric conductivity of material D ($\sigma_D=10^{-2}$ S/m, $\sigma_D=10^{-4}$ S/m). The supply frequency is 1 MHz. In the diagrams, the solid lines represent the standard finite element solution, while the dot lines are the solutions obtained by the homogenization approach with higher order corrector terms.

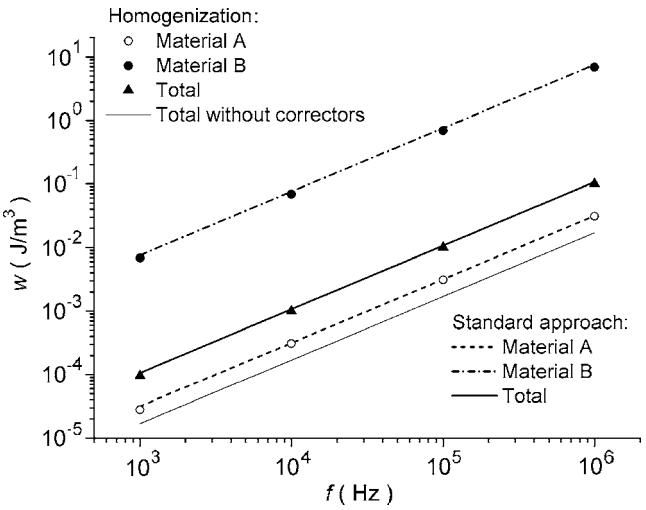

FIG. 13. Joule energy losses per unit volume vs frequency for the electrical conductivity of the layer $\sigma_D = 10^{-2}$ S/m.

ture, are modeled by means of a mathematical homogenization approach based on the multiple scale expansion theory. The interest for this technique is justified by its capability to reproduce, with a limited computational effort, not only average distributions of the field quantities, but also local behaviors modeled thanks to the introduction of higher order correctors.

The attention has been focused on the evaluation of conductive and displacement currents generated by a time varying magnetic flux flowing through a heterogeneous material, having a regular periodic structure composed of ferromagnetic grains dispersed within an insulating lattice. The uniaxial periodicity of layered structures has been also investigated. The results have shown that, depending on the microscopic structure, on the constitutive properties, and on the supply frequency, the induced current distribution can range from a local behavior, with a weak interaction between adjacent grains, to a global evolution, typical of a homogeneous material with "averaged" properties. The homogenization approach has been proven to well reproduce both these physical behaviors, provided that higher order correctors are superposed to the homogenized solution. The great advantage of the proposed approach, with respect to standard numerical methods, is the possibility of analyzing domains constituted by a high number of cells, without a substantial increase of the computational burden.

Future work will be addressed towards two fundamental topics: The first one concerns the theoretical insight of the convergence properties in presence of correctors with order higher than two. The second one refers to the analysis of fine periodic structures in presence of local nonlinear magnetic properties.

[1] L. Rayleigh, Philos. Mag. **34**, 481 (1892).
[2] J. Lam, J. Appl. Phys. **60**, 4230 (1986).
[3] J. C. M. Garnett, Philos. Trans. R. Soc. London, Ser. A **203**, 305 (1904).
[4] R. Landauer, AIP Conf. Proc. **40**, 2 (1978).
[5] J. P. Eberhard, Phys. Rev. E **72**, 036616 (2005).
[6] H. M. Yin and L. Z. Sun, Phys. Rev. B **72**, 054409 (2005).
[7] C. Brosseau and A. A. Beroual, J. Phys. D **34**, 704 (2001).
[8] C. Brosseau, A. Beroual, and A. Boudida, J. Appl. Phys. **88**, 7278 (2000).
[9] K. K. Karkkainen, A. H. Sihvola, and K. I. Nikoskinen, IEEE Trans. Geosci. Remote Sens. **38**, 1303 (2000).
[10] Y. V. Serdyuk, A. D. Podoltsev, and S. M. Gubanski, IEEE Trans. Dielectr. Electr. Insul. **11**, 379 (2004).
[11] V. Myroshnychenko and C. Brosseau, Phys. Rev. E **71**, 016701 (2005).
[12] E. Sanchez-Palencia, *Non-homogenous Media and Vibration Theory* (Springer-Verlag, Berlin, 1980).
[13] C. Conca and S. Natesan, Comput. Methods Appl. Mech. Eng. **192**, 47 (2003).
[14] N. Wellander and G. Kristensson, SIAM J. Appl. Math. **64**, 170 (2003).
[15] D. Trichet, E. Chauveau, and J. Fouladgar, IEEE Trans. Magn. **36**, 1193 (2000).
[16] M. Chiampi and D. Chiarabaglio, IEEE Trans. Magn. **28**, 1917 (1992).
[17] V. V. Jikov, S. M. Kozlov, and O. A. Oleinik, *Homogenization of Differential Operators and Integral Functionals* (Springer-Verlag, Berlin, 1994).
[18] T. A. Suslina, Algebra Anal. **16**, 162 (2004).
[19] C. Beatrice, O. Bottauscio, M. Chiampi, F. Fiorillo, and A. Manzin, J. Magn. Magn. Mater. **304**, e740 (2006).
[20] O. Bottauscio, V. Chiadó Piat, M. Chiampi, M. Codegone, and A. Manzin, IEEE Trans. Magn. **41**, 4060 (2005).